IEEE Access
Multidisciplinary | Rapid Review | Open Access Journal

Received 12 November 2023, accepted 25 November 2023, date of publication 30 November 2023,
date of current version 6 December 2023.

Digital Object Identifier 10.1109/ACCESS.2023.3337810

RESEARCH ARTICLE

SIW-Fed Patch Array Filtenna With Significant Suppression of Adjacent 5G Spectrum for Radio Altimeters

JUNMO CHOI[1], JAEWOO KIM[2], YOUNGGUN JI[2], SEONGJU LEE[2], JUNGRAN LEE[2], BYUNGGIL YU[2], SEULGI PARK[2], MYUNGHO KIM[2], AND KYUNG-YOUNG JUNG[1], (Senior Member, IEEE)

[1]Department of Electronic Engineering, Hanyang University, Seoul 04763, South Korea
[2]Tactical Communication System Team, Hanwha Systems, Seongnam-Si, Gyeonggi-Do 13524, South Korea

Corresponding author: Kyung-Young Jung (kyjung3@hanyang.ac.kr)

This work was supported by the Institute of Civil-Military Technology Cooperation Program funded by the Defense Acquisition Program Administration and Ministry of Trade, Industry and Energy of Korean Government under Grant 9991008134.

ABSTRACT We propose a 2 × 2 patch array filtenna specifically designed for radio altimeter applications with significant suppression of unwanted adjacent 5G spectrum signals. The patch radiator is carefully selected to meet the radiation requirement of radio altimeters and the substrate integrated waveguide (SIW) feeding network is meticulously designed to provide shielding property and excellent suppression level for adjacent 5G spectrum through the evanescent mode characteristic. In specific, the proposed filtenna harnesses inherent suppression characteristic of low-band RF signals below a cutoff frequency in the SIW feeding network, eliminating the need for additional filtering geometries. The proposed filtenna is fabricated and measured, and experimental results confirm its effective operation in the radio altimeter band (4.2–4.4 GHz), exhibiting successful suppression of 5G spectrum (3.4–4 GHz) by 40.70-dB to 43.26-dB. Comparative analysis reveals that the proposed filtenna demonstrates superior suppression level for adjacent spectrums compared to previous planar array filtennas.

INDEX TERMS Filtenna, SIW, radio altimeter.

I. INTRODUCTION

The radio altimeter, an aircraft-mounted radar used to measure absolute altitude during takeoff and landing, demands high reliability [1]. However, with the upcoming extension of the 5G spectrum to 3.7 – 4 GHz (from the current 3.4 – 3.7 GHz) in South Korea, there is growing concern about interference from the adjacent 5G spectrum to the radio altimeter band (4.2 – 4.4 GHz) [2]. This concern is substantiated by a detailed analysis of the safety interference limit outlined in [3]. Additionally, [1] recommends that the interfered signals should be suppressed by up to 40 dB. Therefore, achieving significant suppression of the adjacent 5G spectrum is necessary to ensure the high reliability of radio altimeters.

The associate editor coordinating the review of this manuscript and approving it for publication was Giorgio Montisci.

The conventional approach to suppress a specific spectrum involves cascading a filter at the end of an antenna [4], [5], [6], [7], [8], [9], [10], [11], [12]. However, this approach suffers from mismatch and transmission losses between each component [13]. Moreover, when filtering signals in adjacent spectrums, high-order filters are often cascaded, resulting in significant losses [14], [15].

Recently, a novel concept called the filtering antenna, commonly referred to as a ''filtenna'' was proposed to address the limitations of the traditional approach [16], [17]. The filtenna is an antenna that incorporates filtering geometries in a feed line and/or a radiator. The filtenna effectively reduces mismatch losses by considering the input impedance of a radiator and customizing its filtering geometries [18], [19], [20], [21], [22], [23], [24], [25], [26], [27], [28], [29]. Previous planar array filtennas typically employed band-pass filtering geometries based on resonator coupling principles.

Efforts to enhance suppression, as reported in [20], [23], and [26], involve diverse strategies such as employing loops, L-shaped probes, stubs, symmetric U-shaped hairpin lines, and utilizing current cancellation effects between radiators. Despite these approaches, however, achieving 40 dB suppression of adjacent RF spectrum signals remains highly challenging.

A substrate integrated waveguide (SIW) is a waveguiding structure formed by connecting the upper and lower metal plates of a substrate using periodic via holes [30], [31], [32]. In the context of patch antennas, the SIW feeding network offers several advantages over the microstrip-based feeding network: lower transmission loss, reduction in parasitic radiation, and improvement in shielding properties [33]. Inherently, the SIW feeding network exhibits high-pass filtering characteristics and the cutoff frequency is adjusted by changing the width of the SIW transmission line. Its high-pass filtering characteristics can lead to the evanescent-mode operation of RF signals below the cutoff frequency.

In this work, we propose an innovative filtenna designed for radio altimeters by harnessing the inherent evanescent-mode characteristic of the SIW feeding network to achieve significant suppression of the adjacent 5G spectrum. The proposed filtenna comprises an SIW feeding network and a 2 × 2 patch array radiator. The cutoff frequency of SIW is precisely determined to effectively suppress the 5G spectrum while maintaining good transmission performance within the radio altimeter band. The SIW feeding network is designed to include bends, T-junctions, and slots with the goal of efficiently coupling RF signals in the radio altimeter band with the 2 × 2 patch array radiator and simultaneously maintaining the evanescent-mode characteristic within the adjacent 5G spectrum. It will be shown that the proposed filtenna exhibits remarkable suppression of the adjacent 5G spectrum through the evanescent mode of the SIW feeding network, rendering it highly suitable for radio altimeter applications without additional band-pass filtering geometries. The remainder of this paper is organized as follows: First, we present the design and analysis of the proposed filtenna. Next, we present experimental results and verification of the fabricated filtenna. Finally, we provide concluding remarks.

II. DESIGN & ANALYLSIS

Fig. 1 illustrates the proposed 2 × 2 patch array filtenna, consisting of the 2 × 2 patch array radiator and the SIW feeding network. The overall dimensions of the proposed filtenna are 110 × 160 × 4.064 mm^3. The 2 × 2 patch array radiator is designed on a 3.048 mm thick F4BM substrate ($\epsilon_r = 4.4$, $\tan\delta = 0.0033$) and the SIW feeding network is designed on the same substrate with a thickness of 1.016 mm.

In Fig. 2, the schematic of the 2 × 2 patch array radiator (Substrate 1) is presented. For the operating frequencies ranging from 4.2 GHz to 4.4 GHz, the patch radiators are designed with dimensions of 13.3 mm (L_{patch}) and 34 mm (W_{patch}). To meet the directivity requirement for radio altimeters, the spacing between the patch radiators is set to 40 mm. The outer

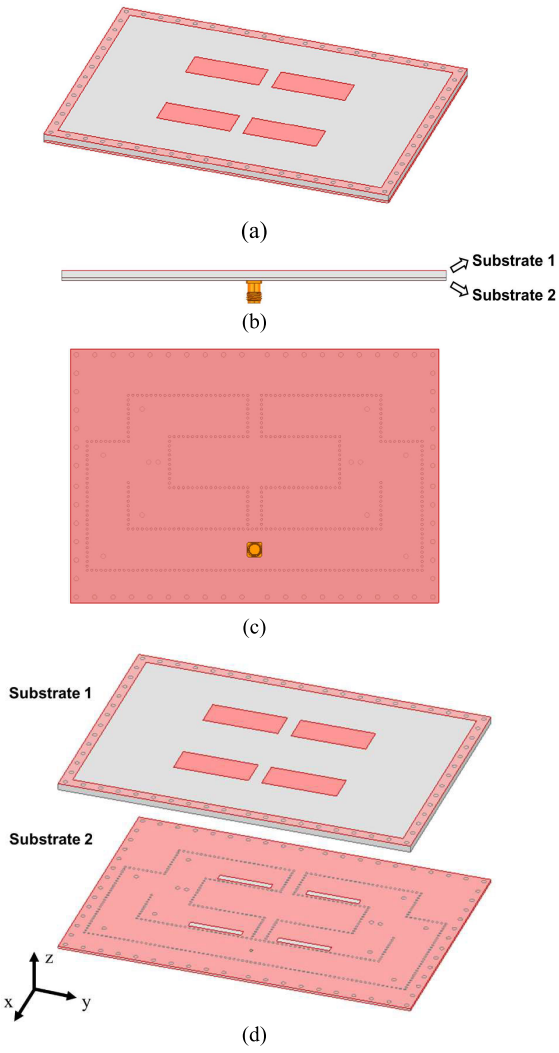

FIGURE 1. Geometry of the proposed 2 × 2 patch array filtenna. (a) Isometric view. (b) Side view. (c) Bottom view. (d) Exploded view.

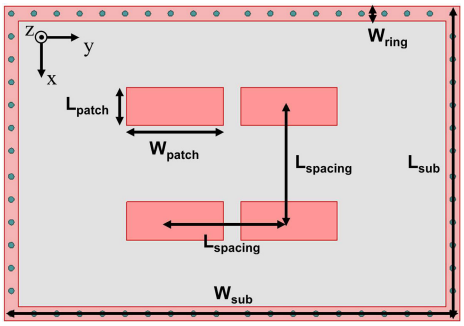

FIGURE 2. Schematic of the 2 × 2 patch array radiator (Substrate 1).

rectangular conductor ring has a width of 5 mm. Within this ring, the via holes with a 1 mm radius and an 8 mm gap are inserted. The final dimensions of the 2 × 2 patch array radiator are summarized in Table 1.

Fig. 3 displays the detailed schematic of the SIW feeding network (Substrate 2). The SIW feeding network is

TABLE 1. Geometrical parameters of the 2 × 2 patch array radiator (Substrate 1).

Parameter	Dimension [mm]	Parameter	Dimension [mm]
L_{patch}	13.3	L_{sub}	110
W_{patch}	34	W_{sub}	160
$L_{spacing}$	40	W_{ring}	5

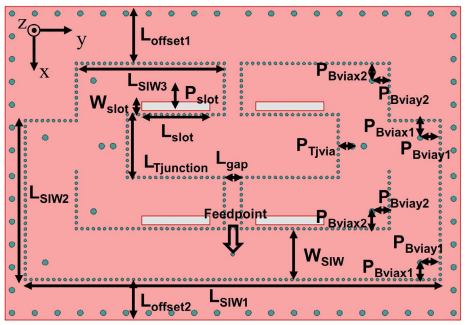

FIGURE 3. Schematic of the SIW feeding network (Substrate 2).

intentionally designed to possess symmetry, ensuring the in-phase coupling of each patch radiator. The filtenna is excited to the center of the SIW transmission line through the 50 Ω SMA connector. The position of the feeding point is determined to split RF signals equally into left and right sides. RF signals excited from the feeding point are efficiently coupled with the 2 × 2 patch array radiator by employing bends, T-junctions, and slots. As a result, this SIW feeding network comprises eight bends, two T-junctions, and four slots, all of which should be optimized for impedance matching with the 2 × 2 patch radiator.

As alluded previously, in the proposed filtenna, the SIW transmission line should be meticulously designed to efficiently guide RF signals in the radio altimeter band, while significantly suppressing the 5G spectrum. The cutoff frequency of the SIW transmission line is determined by the substrate, via holes, and the SIW width (W_{SIW}). In specific, W_{SIW} is calculated by the cutoff frequency as follows [34], [35]:

$$W_{SIW} = \frac{1}{2f_{c10}\sqrt{\mu\varepsilon}} + \frac{d^2}{0.95s} \quad (1)$$

where f_{c10} is the TE_{10} mode cutoff frequency of SIW, d and s denote the diameter of via holes and the center-to-center distance, while ε and μ represent the permittivity and permeability of the substrate, respectively. In this work, via holes with a 1 mm diameter (s) and a 2 mm the center-to-center distance (d) are employed, in accordance with SIW design guidelines [30]. The cutoff frequency (f_{c10}) is set as 4.16 GHz to ensure good transmission performance at 4.2 GHz. Therefore, we choose W_{SIW} as 17.9 mm. Fig. 4 presents the simulated transmission coefficient of the SIW transmission line with respect to W_{SIW}. The simulated SIW transmission line's length is set as 173.65 mm,

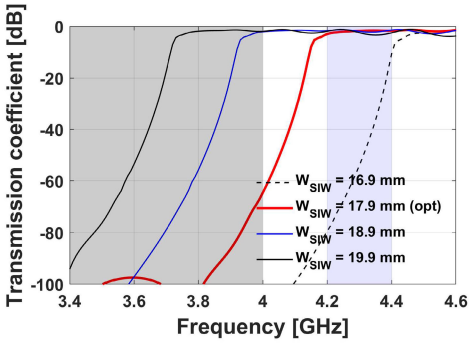

FIGURE 4. Simulated transmission coefficient of the SIW transmission line versus the SIW width (W_{SIW}).

representing the distance between the feeding point and slots. The blue box represents the target operating frequency range for radio altimeters (4.2 – 4.4 GHz), while the gray box indicates the adjacent 5G spectrum to be suppressed. The simulation results indicate that the SIW transmission line, designed with the calculated SIW width, operates effectively in the radio altimeter band but does not function within the 5G spectrum.

Fig. 5 presents the simulated reflection coefficient of the proposed filtenna with respect to the position of via holes for bends (P_{Bviax1} and P_{Bviay1}). The radius of via holes for bends is selected for 1 mm. The position of via holes for bends is chosen to have good reflection coefficient in the range of operating frequencies. The P_{Bviax1} is chosen as 6 mm and the P_{Bviay1} is chosen as 7 mm.

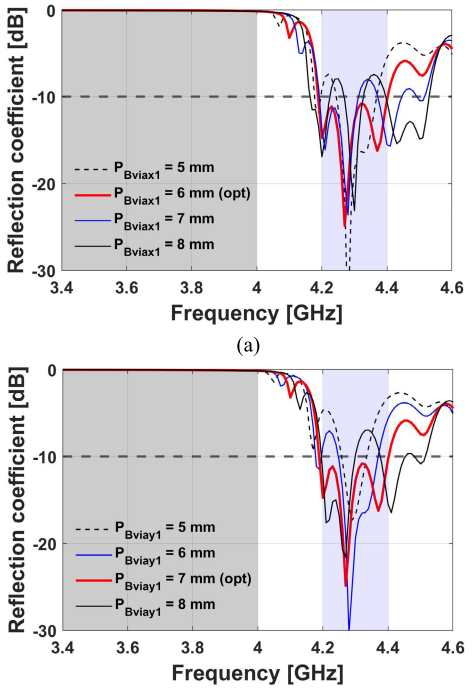

FIGURE 5. Simulated reflection coefficient of the proposed filtenna versus the position of via holes for bends. (a) P_{Bviax1}. (b) P_{Bviay1}.

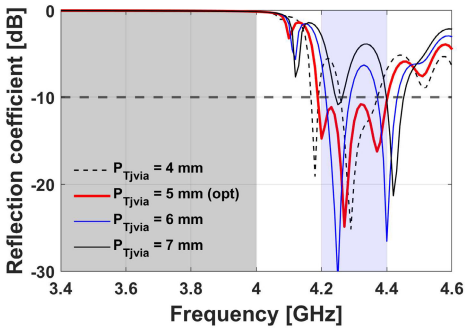

FIGURE 6. Simulated reflection coefficient of the proposed filtenna versus the position of the via holes for T-junctions (P_{Tjvia}).

Fig. 6 displays the simulated reflection coefficient of the proposed filtenna in relation to the position of the via holes for the T-junctions (P_{Tjvia}). The via holes for the T-junctions are specified with a radius of 1 mm, and there is a 4 mm gap between the via holes. The optimal position for the via holes (P_{Tjvia}) is identified as 5 mm, where good impedance matching is achieved. The via holes of bends near the T-junctions are strategically positioned for impedance matching, with the specific parameters P_{Bviax2} and P_{Bviay2} set to 6 mm, distinct from other bends.

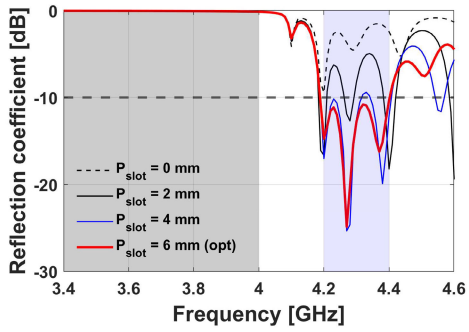

FIGURE 7. Simulated reflection coefficient of the proposed filtenna versus the position of slots (P_{slot}).

Fig. 7 presents the simulated reflection coefficient of the proposed filtenna as a function of the position of slots (P_{slot}) which is defined as the intercenter distance between the SIW and slots. As shown in the figure, the optimal position of slots (P_{slot}) is determined to be 6 mm, enabling optimized impedance matching within the operating frequency range. In addition, other slot parameters are carefully chosen to achieve favorable reflection coefficients. The width of the slot (W_{slot}) is set at 3 mm, and its length (L_{slot}) is chosen as 24 mm. To precisely position the slots at the center of each patch radiator, $L_{offset1}$ and $L_{offset2}$ are set as 20.05 mm and 14.15 mm, respectively. The remaining parameters are optimized in a similar fashion: $L_{gap} = 6$ mm, $L_{SIW1} = 145.6$ mm, $L_{SIW2} = 55.8$ mm, $L_{SIW3} = 51.9$ mm, and $L_{Tjunction} = 22.1$ mm. The final dimensions of the SIW feeding network (Substrate 2) are summarized in Table 2. Finally, the simulated reflection coefficient of the proposed filtenna is below –10 dB in the frequency range from 4.19 GHz to 4.4 GHz, meeting the requirement for radio altimeters.

TABLE 2. Geometrical parameters of the SIW feeding network (Substrate 2).

Parameter	Dimension [mm]	Parameter	Dimension [mm]
W_{slot}	3	P_{Bviax2}	6
L_{slot}	24	P_{Bviay2}	6
P_{slot}	6	W_{SIW}	17.9
P_{Bviax1}	6	L_{SIW1}	145.6
P_{Bviay1}	7	L_{SIW2}	55.8
P_{Tjvia}	5	L_{SIW3}	51.9
$L_{Tjunction}$	22.1	$L_{offset1}$	20.05
L_{gap}	6	$L_{offset2}$	14.15

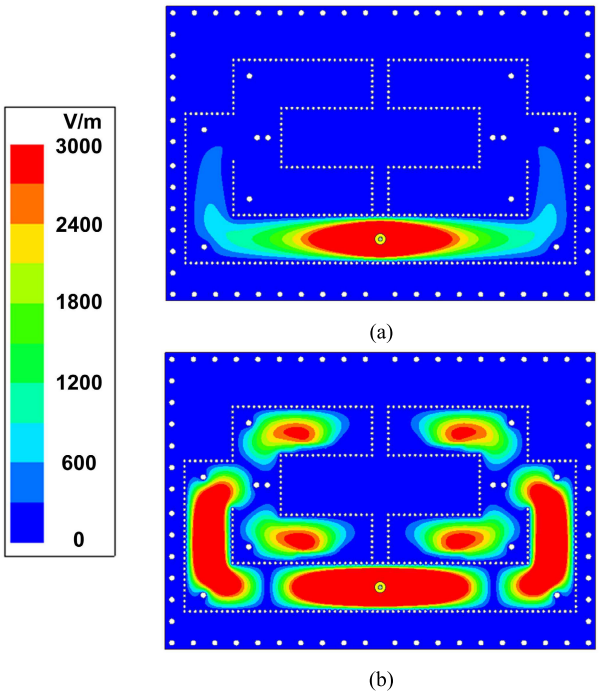

FIGURE 8. Electric field distribution of the SIW feeding network. (a) 4 GHz. (b) 4.2 GHz.

Fig. 8 illustrates the electric field distributions inside the SIW feeding network at 4 GHz and 4.2 GHz. As shown in the electric field distribution at 4 GHz (Fig. 8(a)), the RF signal below the cutoff frequency cannot propagate due to its evanescent-mode characteristic, resulting in negligible electric fields near slots for coupling the patch radiators. This evanescent-mode behavior is even more pronounced for frequencies below 4 GHz, contributing to the significant suppression of the adjacent 5G spectrum. Meanwhile, as depicted in the electric field distribution at 4.2 GHz (Fig. 8(b)), the RF signal operate in the propagating TE_{10} mode and

effectively couple with the patch radiators through all slots in the SIW feeding network. Consequently, RF signals in the radio altimeter band efficiently radiate through the patch radiators.

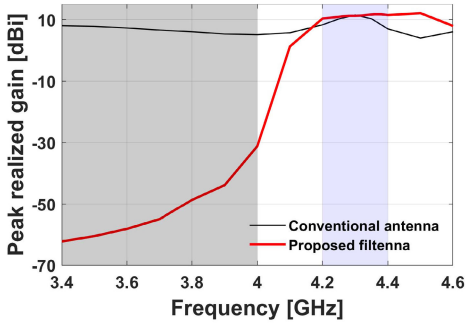

FIGURE 9. Simulated peak realized gain versus the frequency.

Fig. 9 illustrates the simulated peak realized gain versus the frequency for the proposed filtenna. For comparison, a conventional antenna—specifically, the 2 × 2 patch array antenna with a microstrip-based feeding network depicted in Figure 1 of [36]—is designed on a 3.048 mm thick F4BM substrate (same as the proposed filtenna). The conventional antenna exhibits a simulated realized gain ranging from 7.57 to 11.46 dBi in the radio altimeter band and a simulated realized gain ranging from 5.21 to 7.34 dBi in the adjacent 5G spectrum. Despite the patch antenna's narrow bandwidth characteristic, its realized gain is decreased slightly in the adjacent 5G spectrum. Conversely, the proposed filtenna exhibits a realized gain ranging from 10.01 to 11.37 dBi in the radio altimeter band, significantly dropping to –31.34 to –66.00 dBi in the adjacent 5G spectrum. Consequently, the conventional antenna's suppression level in the adjacent 5G spectrum is ranging from 4.12 to 6.25 dB, whereas the proposed filtenna achieves notably higher suppression, ranging from 42.71 to 77.37 dB. This suppression level is calculated as the difference between the highest realized gain in the radio altimeter band and the realized gain in the 5G spectrum. Both the proposed filtenna and the conventional antenna have similar peak realized gain in the radio altimeter band. However, unlike the conventional antenna with the microstrip feeding network, the proposed filtenna with the SIW feeding network, operating specifically in the evanescent-mode characteristic at the 5G spectrum, effectively suppresses adjacent 5G signals. The simulation results demonstrate that the proposed filtenna achieves good radiation in the radio altimeter band while efficiently suppressing RF signals in the adjacent 5G spectrum thanks to our simple yet intelligent feeding network approach.

III. MEASUREMENT & VERIFICATION

Fig. 10 displays the fabricated filtenna and the antenna measurement setup within an anechoic chamber. Fig. 11 illustrates the simulated and measured reflection coefficients

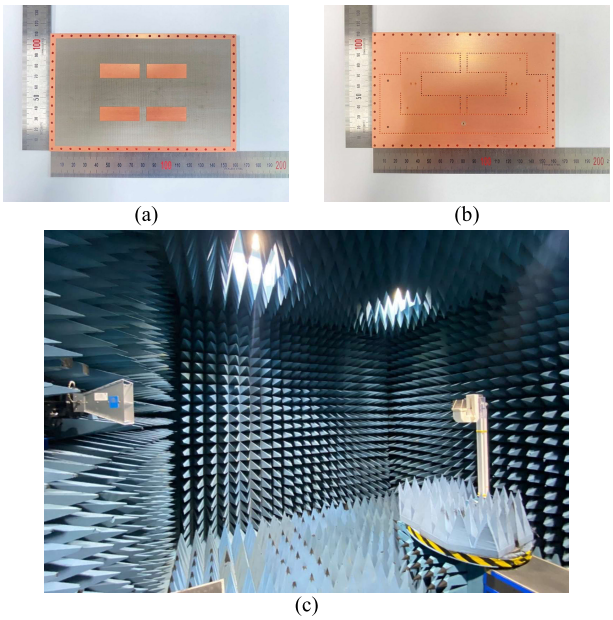

FIGURE 10. Fabricated filtenna and measurement setup. (a) Top view of the fabricated filtenna. (b) Bottom view of the fabricated filtenna. (c) Measurement setup.

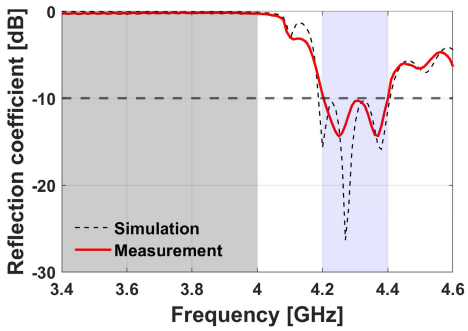

FIGURE 11. Simulated and measured reflection coefficients of the proposed filtenna.

of the proposed filtenna. Notably, the measured reflection coefficient remains below –10 dB across the frequency range of 4.20 GHz to 4.40 GHz, which agrees well with the simulated results. As a result, the fabricated filtenna successfully meets the required operating frequencies for radio altimeters.

The simulated and measured peak realized gains of the proposed filtenna are presented in Fig. 12. Across the operating frequency range, the measured peak realized gain ranges from 8.06 dBi to 9.17 dBi. The observed difference between the simulated and measured peak realized gain may be attributed to fabrication and measurement errors. In the adjacent 5G band, the measured peak realized gain of the fabricated filtenna ranges from –31.53 dBi to –34.09 dBi which is much higher than the simulation result. The disparity between the simulated and measured peak realized gain in this frequency band can be attributed to the limitations in

TABLE 3. Performance comparison of the proposed filtenna with previous planar array filtennas in the literature.

Ref.	Operating frequency	Size ($\lambda_0 \times \lambda_0$)	Layer	Shielding	Radiator	Feeding network	Minimum Suppression level
This work	4.20 – 4.40 GHz	1.57 × 2.14	2	O	Patch	SIW	40.70
[18]	3.45 – 3.55 GHz	Not presented	1	O	Patch	Microstrip	23.1
[19]	27.15 – 28.55 GHz	3.08 × 2.52	3	O	Patch	SIW	15
[20]	5.13 – 5.35 GHz	1.39 × 1.25	2	X	Patch	Microstrip	22
[21]	2.60 – 3.40 GHz	1.40 × 2.00	3	X	Patch	Microstrip	30
[22]	26.87 – 27.35 GHz	2.62 × 1.59	1	O	Slot	SIW	26
[23]	23.50 – 31.50 GHz	2.66 × 2.20	4	O	Patch	SIW	29
[24]	9.83 – 10.19 GHz	2.00 × 0.67	1	X	Patch	Microstrip	30
[25]	9.20 – 10.91 GHz	3.70 × 3.70	2	O	Patch	SIW	33
[26]	57.50 – 66.60 GHz	3.40 × 3.40	2	O	Patch	SIW	27
[27]	13.35 – 13.91 GHz	1.66 × 1.80	2	X	Patch	SIW	13
[28]	13.01 – 13.44 GHz	1.74 × 0.59	2	X	Patch	SIW	22
[29]	13.32 – 13.88 GHz	0.88 × 0.88	2	X	Patch	SIW	27.5

※ λ_0 is the free-space wavelength of the center operating frequency.

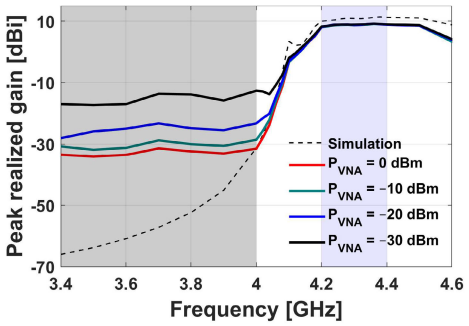

FIGURE 12. Simulated and measured peak realized gains of the proposed filtenna.

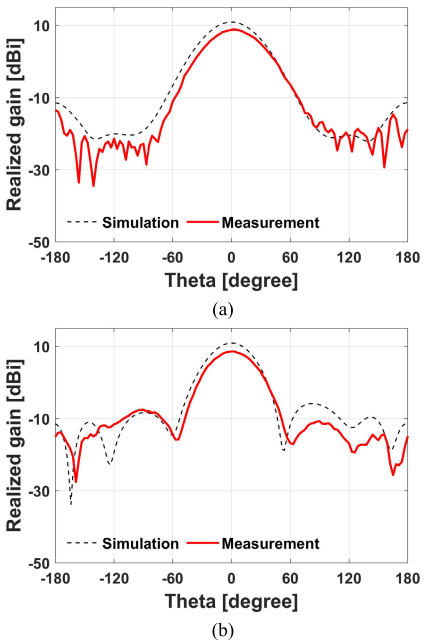

FIGURE 13. Simulated and measured radiation patterns of the proposed filtenna at 4.3 GHz. (a) Azimuth plane (yz-plane). (b) Elevation plane (xz-plane).

measurement performance. To address this issue, additional measurements are performed for various input power levels of the vector network analyzer (VNA). At 4 GHz, the peak realized gain for the input power level of –30 dBm, –20 dBm, –10 dBm, and 0 dBm is –12.64 dBi, –24.74 dBi, –28.61 dBi, and –31.53 dBi, respectively. Consequently, due to the limited measurable power level in our measurement facility, the suppression level does not match the simulated counterpart. For the 0 dBm power level, the measured suppression level of the adjacent 5G spectrum is 40.70 dB to 43.26 dB. Despite the constraints of our measurement performance, the measured suppression level of the fabricated filtenna exceeds the 40 dB threshold recommended by ITU-R M.2059.0 [1].

Fig. 13 displays the simulated and measured radiation patterns of the proposed filtenna at 4.3 GHz. The simulated –3 dB beamwidths are 48.90° in the azimuth plane and 49.08° in the elevation plane, while the measured –3 dB beamwidths are 47.18° in the azimuth plane and 41.62° in the elevation plane. Notably, the measured –3 dB beamwidth fulfills the requirements for radio altimeters [1].

Table 3 presents a performance comparison between the proposed filtenna and previous planar array filtennas in the literature. The conventional filtennas in the table utilize couplings between resonators or transmission lines as their fundamental approach, and some of them employ additional or modified geometries to enhance suppression level. For example, [20], [23], and [26] utilize current cancellation effects between radiators, [23] employs loops, L-shaped probes, and stubs, and [26] exploits two symmetric U-shaped hairpin lines. As highlighted in Table 3, our proposed filtenna employing the evanescent-mode characteristic excels in achieving superior suppression level compared to previous works based on the band-pass filtering geometries. Moreover, [20], [21], [24], [27], [28], and [29] lacked the shielding characteristic. In summary, our proposed filtenna leverages the intelligent SIW feeding network without additional filtering geometries, offering high-performance filtering and shielding characteristics.

IV. CONCLUDING REMARKS

In this study, we address the critical challenge of potential interference between the expanding 5G spectrum and the radio altimeter band, essential for aviation safety. By ingeniously harnessing inherent suppression characteristics of RF signals below the cutoff frequency within the SIW feeding network, we develop the novel filtenna configuration that achieves remarkable suppression of the adjacent 5G spectrum without resorting to additional filtering geometries. The proposed filtenna design, featuring a 2×2 patch array radiator coupled with the SIW feeding network, demonstrates promising potential for radio altimeter applications. Through meticulous optimization and precise engineering, the proposed filtenna meets the requirements by ITU-R M.2059.0. Our approach stands out from prior works by leveraging the SIW feeding network's unique evanescent-mode and shielding characteristics. This strategic integration eliminates the need for complex band-pass filtering components, ultimately contributing to the simplicity and effectiveness of our work. The measurement results validate the filtenna's capabilities, with good agreement with simulated results in reflection coefficient, realized gain, and radiation patterns. Despite measurement limitations, our proposed filtenna exhibits excellent performance, meeting crucial operational requirements for radio altimeters. Therefore, we present the SIW-fed patch array filtenna as a promising solution for radio altimeters, effectively suppressing the adjacent 5G spectrum.

REFERENCES

[1] *Operational and Technical Characteristics and Protection Criteria of Radio Altimeters Utilizing the Band 4 200–4 400 MHz*, document ITU-R M.2059-0, Feb. 2014.
[2] S. Liu, J. Li, S.-H. Hwang, H.-K. Son, and Y.-J. Chong, "Interference analysis method for 5G system to radio altimeter," in *Proc. IEEE VTS Asia–Pacific Wireless Commun. Symp. (APWCS)*, Seoul, South Korea, Aug. 2022, pp. 80–84.
[3] *Assessment of C-Band Mobile Telecommunications Interference Impact on Low Range Radar Altimeter Operations*. Accessed: Oct. 10, 2023. [Online]. Available: https://www.rtca.org/wp-content/uploads/2020/10/SC-239-5G-Interference-Assessment-Report_274-20-PMC-2073_accepted_changes.pdf
[4] J.-S. Hong and M. J. Lancaster, *Microstrip Filters for RF/Microwave Applications*, 2nd ed. Hoboken, NJ, USA: Wiley, 2011.
[5] A. Basit, M. I. Khattak, M. Al-Hasan, J. Nebhen, and A. Jan, "Design and analysis of a compact GSM/GPS dual-band bandpass filter using a T-shaped resonator," *J. Electromagn. Eng. Sci.*, vol. 22, no. 2, pp. 138–145, Mar. 2022.
[6] G. Chaudhary and Y. Jeong, "A tunable bandpass filter with arbitrarily terminated port impedance using dual-mode resonator," *J. Electromagn. Eng. Sci.*, vol. 22, no. 6, pp. 647–655, Nov. 2022.
[7] P. Pech, P. Kim, G. Chaudhary, and Y. Jeong, "Substrate integrated waveguide quasi-elliptic filter with arbitrary termination impedances," *J. Electromagn. Eng. Sci.*, vol. 22, no. 4, pp. 472–478, Jul. 2022.
[8] A. Sowjanya and D. Vakula, "Compact dual bandpass filter using dual-split ring resonator for 5G upper microwave flexible use services," *J. Electromagn. Eng. Sci.*, vol. 22, no. 4, pp. 434–439, Jul. 2022.
[9] A. Basit, M. I. Khattak, A. Althuwayb, and J. Nebhen, "Compact triband bandpass filter based on asymmetric step impedance resonators for WiMAX and RFID systems," *J. Electromagn. Eng. Sci.*, vol. 21, no. 4, pp. 316–321, Sep. 2021.
[10] K.-D. Xu, Y.-J. Guo, Y. Liu, X. Deng, Q. Chen, and Z. Ma, "60-GHz compact dual-mode on-chip bandpass filter using GaAs technology," *IEEE Electron Device Lett.*, vol. 42, no. 8, pp. 1120–1123, Aug. 2021.
[11] X. Huang, X. Zhang, L. Zhou, J.-X. Xu, and J.-F. Mao, "Low-loss self-packaged Ka-band LTCC filter using artificial multimode SIW resonator," *IEEE Trans. Circuits Syst. II, Exp. Briefs*, vol. 70, no. 2, pp. 451–455, Feb. 2023.
[12] B. Xu and Y. Guo, "A novel DVL calibration method based on robust invariant extended Kalman filter," *IEEE Trans. Veh. Technol.*, vol. 71, no. 9, pp. 9422–9434, Sep. 2022.
[13] W.-J. Wu, Y.-Z. Yin, S.-L. Zuo, Z.-Y. Zhang, and J.-J. Xie, "A new compact filter-antenna for modern wireless communication systems," *IEEE Antennas Wireless Propag. Lett.*, vol. 10, pp. 1131–1134, 2011.
[14] F. Zhu, G. Q. Luo, B. You, X. H. Zhang, and K. Wu, "Planar dual-mode bandpass filters using perturbed substrate-integrated waveguide rectangular cavities," *IEEE Trans. Microw. Theory Techn.*, vol. 69, no. 6, pp. 3048–3057, Jun. 2021.
[15] S. Li and Z. Zhang, "Compact multi-order bandpass filter with high stopband rejection performance," *Electron. Lett.*, vol. 55, no. 12, pp. 701–703, Jun. 2019.
[16] Y. Sung, "Simple patch antenna with filtering function using two U-slots," *J. Electromagn. Eng. Sci.*, vol. 21, no. 5, pp. 425–429, Nov. 2021.
[17] J. Choi, S. Park, J. Lee, and K.-Y. Jung, "UHF-printed monopole filtenna for partial discharge detection with LTE signal suppression," *J. Electromagn. Eng. Sci.*, vol. 23, no. 2, pp. 180–187, Mar. 2023.
[18] F.-C. Chen, H.-T. Hu, R.-S. Li, Q.-X. Chu, and M. J. Lancaster, "Design of filtering microstrip antenna array with reduced sidelobe level," *IEEE Trans. Antennas Propag.*, vol. 65, no. 2, pp. 903–908, Feb. 2017.
[19] H. Jin, G. Q. Luo, W. Wang, W. Che, and K.-S. Chin, "Integration design of millimeter-wave filtering patch antenna array with SIW four-way antiphase filtering power divider," *IEEE Access*, vol. 7, pp. 49804–49812, 2019.
[20] G. Liu, Y. M. Pan, and X. Y. Zhang, "Compact filtering patch antenna arrays for marine communications," *IEEE Trans. Veh. Technol.*, vol. 69, no. 10, pp. 11408–11418, Oct. 2020.

[21] Y.-M. Zhang, S. Zhang, G. Yang, and G. F. Pedersen, "A wideband filtering antenna array with harmonic suppression," *IEEE Trans. Microw. Theory Techn.*, vol. 68, no. 10, pp. 4327–4339, Oct. 2020.
[22] Y.-X. Yan, W. Yu, and J.-X. Chen, "Millimeter-wave low side- and back-lobe SIW filtenna array fed by novel filtering power divider using hybrid TE101/TE301 mode SIW cavities," *IEEE Access*, vol. 9, pp. 167706–167714, 2021.
[23] H.-T. Hu and C. H. Chan, "Substrate-integrated-waveguide-fed wideband filtering antenna for millimeter-wave applications," *IEEE Trans. Antennas Propag.*, vol. 69, no. 12, pp. 8125–8135, Dec. 2021.
[24] S. Ji, Y. Dong, and Y. Fan, "Bandpass filter prototype inspired filtering patch antenna/array," *IEEE Trans. Antennas Propag.*, vol. 70, no. 5, pp. 3297–3307, May 2022.
[25] W. Wang, H. Jin, W. Yu, X. H. Zhang, K.-S. Chin, and G. Q. Luo, "A wideband circularly polarized 2 × 2 filtenna array with multiple radiation nulls," *IEEE Antennas Wireless Propag. Lett.*, vol. 21, no. 3, pp. 595–599, Mar. 2022.
[26] H.-T. Hu, K. F. Chan, and C. H. Chan, "60 GHz Fabry–Pérot cavity filtering antenna driven by an SIW-fed filtering source," *IEEE Trans. Antennas Propag.*, vol. 70, no. 2, pp. 823–834, Feb. 2022.
[27] S.-C. Tang, X.-Y. Wang, W. Yu, W.-W. Yang, and J.-X. Chen, "Compact microstrip patch filtenna array based on reusable high-order SIW cavity," *IEEE Antennas Wireless Propag. Lett.*, vol. 22, no. 2, pp. 268–272, Feb. 2023.
[28] Y.-X. Yan, Y.-X. Huang, S.-C. Tang, and J.-X. Chen, "Low-sidelobe microstrip patch filtenna array fed by higher-order mode SIW cavity," *IEEE Antennas Wireless Propag. Lett.*, vol. 22, no. 8, pp. 1873–1877, Aug. 2023.
[29] Y.-X. Huang, Y.-X. Yan, S.-C. Tang, W. Yu, and J.-X. Chen, "Substrate-integrated-waveguide-fed slotted patch filtering antenna and array with enhanced selectivity," *AEU Int. J. Electron. Commun.*, vol. 172, Dec. 2023, Art. no. 154936.
[30] A. O. Nwajana and E. R. Obi, "A review on SIW and its applications to microwave components," *Electronics*, vol. 11, no. 7, p. 1160, Apr. 2022.
[31] A. Kumar and S. I. Rosaline, "Hybrid half-mode SIW cavity-backed diplex antenna for on-body transceiver applications," *Appl. Phys. A, Solids Surf.*, vol. 127, no. 11, p. 834, Nov. 2021.
[32] A. Kumar and S. Raghavan, "Planar cavity-backed self-diplexing antenna using two-layered structure," *Prog. Electromagn. Res. Lett.*, vol. 76, pp. 91–96, 2018.
[33] T. Mikulasek, A. Georgiadis, A. Collado, and J. Lacik, "2 × 2 microstrip patch antenna array fed by substrate integrated waveguide for radar applications," *IEEE Antennas Wireless Propag. Lett.*, vol. 12, pp. 595–599, 2013.
[34] Y. Cassivi, L. Perregrini, P. Arcioni, M. Bressan, K. Wu, and G. Conciauro, "Dispersion characteristics of substrate integrated rectangular waveguide," *IEEE Microw. Wireless Compon. Lett.*, vol. 12, no. 9, pp. 333–335, Sep. 2002.
[35] F. Xu and K. Wu, "Guided-wave and leakage characteristics of substrate integrated waveguide," *IEEE Trans. Microw. Theory Techn.*, vol. 53, no. 1, pp. 66–73, Jan. 2005.
[36] K.-S. Chin, H.-T. Chang, J.-A. Liu, H.-C. Chiu, J. S. Fu, and S.-H. Chao, "28-GHz patch antenna arrays with PCB and LTCC substrates," in *Proc. Cross Strait Quad-Regional Radio Sci. Wireless Technol. Conf.*, vol. 1, Jul. 2011, pp. 355–358.

JUNMO CHOI received the B.S. degree from the School of Electronic and Information Engineering, Korea Aerospace University, Goyang, South Korea, in 2021. He is currently pursuing the Ph.D. degree in electronic engineering with Hanyang University, Seoul, South Korea. His current research interests include filtering antennas, circularly polarized antennas, and mmWave antennas.

JAEWOO KIM received the B.S. and M.S. degrees from Hanyang University, Seoul, South Korea, in 1996 and 2009, respectively. From 1996 to 2005, he developed ASICs for QAM and OFDM modems with the Samsung Electronics Research Institute. From 2005 to 2010, he worked on SOC development for mWimax with Postdata. Since 2010, he has been involved in the development of military TICN modems, tactical radios, and tactical mobile communication systems (TMCS) with Hanwha Systems. His research interests include spectrum efficiency, 5G specialized networks, tactical mobile communication, and 6G NTN.

YOUNGGUN JI received the B.E. and M.S. degrees in electronics engineering from Inha University, South Korea, in 2006 and 2008 respectively. He is currently the Chief Engineer of the Tactical Communication System Team, Hanwha Systems. His research interest includes 5G/B5G communications, such as MIMO, NTN, dynamic spectrum sharing, and cognitive radio systems. He was a recipient of the Best Paper Award from the *Journal of Communications and Networks* (JCN) of KICS, in 2007.

SEONGJU LEE received the M.S. degree in information and communication engineering from Kyungnam University, South Korea, in 2003. From 2003 to 2005, he was with the Plasma Technologies Center, Institute for Advanced Engineering, working on high-power transmitters for satellite communication systems. He is currently a Senior Engineer with the Tactical Communication System Team, Hanwha Systems. His research interests include mmWave, RF, and mixed-signal circuit design for wireless communication systems.

JUNGRAN LEE received the M.S. degree from the School of Telecommunication Engineering, Jeju National University, Jeju, South Korea, in 2000. She is currently with Hanwha Systems, Seoul, South Korea. Her current research interest includes tactical communication systems.

BYUNGGIL YU received the Ph.D. degree in radio engineering from Kwangwoon University, South Korea, in 2010. He is currently the Chief Engineer of the Tactical Communication System Team, Hanwha Systems, South Korea. His research interests include active phased array antenna for wireless communication, antenna optimization algorithms, and metamaterial.

SEULGI PARK received the B.S. and M.S. degrees in electrical engineering from Hongik University, South Korea, in 2006 and 2008, respectively. From 2008 to 2013, he was with the Electronic Warfare Research Center, LIG Nex1 Corporation. From 2013 to 2016, he was with the DMC Research Center, Samsung Electronics Corporation. Since January 2017, he has been with the Tactical Communication System Team, Hanwha Systems. His major research interests include electronic warfare transmission/reception antennas, electronic warfare systems, and tactical communication systems.

MYUNGHO KIM received the B.E. and M.S. degrees in electronics engineering from Kyung Hee University, South Korea, in 2002 and 2004, respectively. He is currently the Chief Engineer with the Tactical Communication System Team, Hanwha Systems. His research interest includes 5G/B5G communications, such as MIMO, NTN, and cognitive radio systems.

KYUNG-YOUNG JUNG (Senior Member, IEEE) received the B.S. and M.S. degrees in electrical engineering from Hanyang University, Seoul, South Korea, in 1996 and 1998, respectively, and the Ph.D. degree in electrical and computer engineering from The Ohio State University, Columbus, OH, USA, in 2008.

From 2008 to 2009, he was a Postdoctoral Researcher with The Ohio State University. From 2009 to 2010, he was an Assistant Professor with the Department of Electrical and Computer Engineering, Ajou University, Suwon, South Korea. Since 2011, he has been with Hanyang University, where he is currently a Professor with the Department of Electronic Engineering. His current research interests include computational electromagnetics, bioelectromagnetics, and nano-electromagnetics.

Dr. Jung was a recipient of the Graduate Study Abroad Scholarship from the National Research Foundation of Korea, the Presidential Fellowship from The Ohio State University, the HYU Distinguished Teaching Professor Award from Hanyang University, and the Outstanding Research Award from the Korean Institute of Electromagnetic Engineering and Science.